

# Theory of Heavy Flavor in the Quark-Gluon Plasma

Ralf Rapp

*Cyclotron Institute and Department of Physics and Astronomy, Texas A&M University, College Station, TX 77843-3366, U.S.A.*

---

## Abstract

Heavy-quark interactions in the Quark-Gluon Plasma are analyzed in terms of a selfconsistent Brueckner scheme using a thermodynamic  $T$ -matrix based on a potential model. The interrelations between quarkonium correlators, spectral functions and zero-modes, and open heavy-flavor transport and susceptibilities are elaborated. Independent constraints from thermal lattice QCD can be used to improve predictions for heavy-quark phenomenology in heavy-ion collisions.

*Key words:* Quark-gluon plasma, heavy quarks, Brueckner theory

*PACS:* 25.75.Nq, 14.40.Pq, 14.65.Dw, 24.10.Cn

---

## 1. Introduction

A basic challenge in many-body physics is the understanding of matter properties in terms of the forces between the constituents. Medium modifications of the force (or potential) render its determination an additional challenge. It is therefore important to have a good control over the force at least in the vacuum. In Quantum Chromodynamics (QCD), the fundamental force between static charges, i.e., a heavy quark ( $Q$ ) and antiquark ( $\bar{Q}$ ), is well established, both theoretically and phenomenologically. The heavy-quark (HQ) potential has been extracted with high accuracy from lattice-QCD (lQCD) computations [1] and can be well represented by the so-called Cornell potential,

$$V_{Q\bar{Q}}(r) = -\frac{4}{3} \frac{\alpha_s}{r} + \sigma r , \quad (1)$$

characterized by a perturbative color-Coulomb interaction at small distances and a “string” term dominant at large  $r$ , cf. left panel of Fig. 1. This potential successfully describes charmonium and bottomonium spectroscopy in vacuum, which can be understood as an effective field theory (EFT) of QCD in a  $1/m_Q$  expansion ( $m_Q$ : HQ mass). The string tension,  $\sigma \simeq 1 \text{ GeV/fm}$ , is of nonperturbative origin and most likely associated with the gluon-condensate structure of the QCD vacuum. The string term plays an

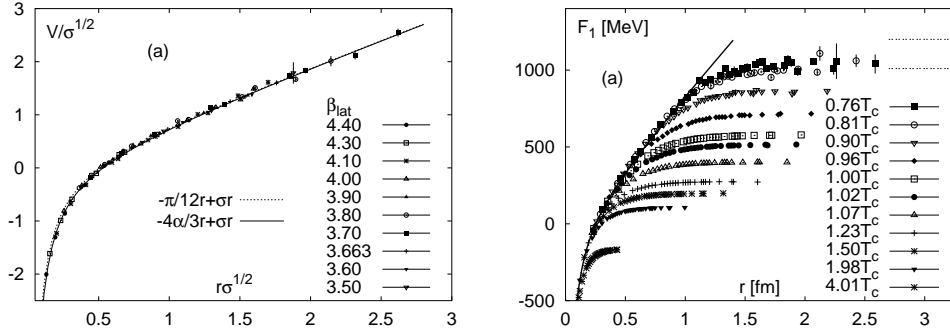


Fig. 1. The static heavy-quark potential in vacuum (left)[1] and the color-singlet free energy in medium (right; reprinted with permission from [2]) as “measured” in lattice QCD as a function of  $Q$ - $\bar{Q}$  separation.

important role already at rather small distances; e.g., for  $V(r_0)=0$ , i.e., at  $r_0 \simeq \frac{1}{4}$  fm, it is equal in magnitude (but opposite in sign) to the Coulomb term. Consequently, the charmonium spectrum is largely governed by the nonperturbative force (e.g., the ground-state binding,  $E_B^{J/\psi} \simeq 0.6$  GeV, collapses to  $\sim 0.05$  GeV if the string term is switched off). With a “calibrated” strong force in vacuum at hand one can study its medium modifications and infer from these information about the phase structure and transport properties of QCD matter. The analysis of quarkonium production and heavy-flavor spectra in ultra-relativistic heavy-ion collisions (URHICs) is aimed at precisely at these objectives, i.e., to identify signals of deconfinement and to extract heavy-quark diffusion coefficients from the produced medium (see, e.g., Refs. [3–6] for recent reviews).

The HQ free energy has also been computed at finite temperature, cf. right panel of Fig. 1. One observes a gradual penetration of medium effects to smaller distances, naturally interpreted as a decrease of the “Debye” screening length,  $r_D \sim 1/m_D$  ( $m_D$ : Debye mass). However, even at temperatures as high as  $2T_c \approx 350$  MeV, the free energy still levels off at a positive value indicative for nonperturbative effects (string term). The applicability of the potential approach requires the 4-momentum transfer to be dominantly spacelike, i.e.,  $q_0 \simeq \vec{q}^2/2m_Q \ll |\vec{q}|$ . In the vacuum this is satisfied by the smallness of the quarkonium binding energy. In the medium the latter is expected to decrease further. The thermal momentum scale of a single heavy quark also remains parametrically large not too far above  $T_c$ ,  $p_{th}^2 \simeq 2m_Q T \gg T^2$  ( $T^2$ : momentum transfer from the medium). Thus, thermal  $Q$ - $\bar{Q}$  and  $Q$ -medium interactions are essentially static and elastic but involve nonperturbative interactions. This suggests the possibility of a unified description of heavy quarkonia and heavy-flavor transport, with a simultaneous treatment of bound and scattering states including resummations. The thermodynamic  $T$ -matrix approach, which is based on potential interactions, is such a framework, and has been successfully applied to electromagnetic plasmas [7]. The in-medium QCD interaction is, of course, much more involved than in QED, but the idea of using input from lQCD has revived the potential approach in recent years [8,3]. In this paper we will elaborate on the  $T$ -matrix approach for open and hidden heavy flavor in the QGP (Sec. 2), and how numerical results for spectral and correlation functions, as well as transport coefficients, can be tested by thermal lQCD (Sec. 3). We conclude in Sec. 4.

## 2. One- and Two-Body Correlations in the QGP

The commonly studied quantity in thermal lattice QCD characterizing the propagation of a hadronic current with quantum numbers  $\alpha$  is the imaginary-time ( $\tau$ ) correlation function which is given by a thermal expectation value as

$$G_\alpha(\tau, \vec{r}) = \langle \langle j_\alpha(\tau, \vec{r}) j_\alpha^\dagger(0, \vec{0}) \rangle \rangle = \text{diagram 1} + \text{diagram 2} . \quad (2)$$

The second equality is a diagrammatic representation for a meson state in terms of its free quark-antiquark loop and a 2-body interaction term. The physical information on the excitation spectrum in that channel is given by the spectral function in momentum space,  $\rho_\alpha(E, p) = -2 \text{Im } G_\alpha^R(E, p)$ . It is related to the euclidean correlator, Eq. (2), via

$$G_\alpha(\tau, p; T) = \int_0^\infty \frac{dE}{2\pi} \rho_\alpha(E, p; T) \frac{\cosh[E(\tau - 1/2T)]}{\sinh[E/2T]} , \quad (3)$$

which illustrates the difficulty in extracting spectral functions from lQCD “data” of the euclidean correlator, since the latter is only obtained for a finite number of  $\tau$ -points on a finite interval,  $0 < \tau < \frac{1}{2T}$ . However, using model calculations for the spectral function a straightforward comparison to lQCD data can be performed and constraints evaluated. Note that the energy integration encompasses both bound and continuum states. Within a HQ potential framework, the  $T$ -matrix formalism is thus an ideal choice [9–11].

Let us first focus on the quarkonium ( $Q\bar{Q}$ ) sector. In ladder approximation, and after partial-wave expansion, the in-medium  $T$ -matrix takes the form [10,11]

$$T_\alpha(E; q', q) = \mathcal{V}_\alpha(q', q) + \frac{2}{\pi} \int_0^\infty dk k^2 \mathcal{V}_\alpha(q', k) G_{Q\bar{Q}}^0(E; k) T_\alpha(E; k, q) , \quad (4)$$

where  $\mathcal{V}_\alpha$  denotes the momentum-space potential and  $G_{Q\bar{Q}}^0$  the uncorrelated 2-particle propagator (the first diagram in Eq. (2)); its imaginary part can be expressed via the in-medium single quark and anti-quark spectral functions,  $\rho_Q$  and  $\rho_{\bar{Q}}$ , as [12]

$$\text{Im } G_{Q\bar{Q}}^0(E, k) = - \int \frac{d\omega}{2\pi} \left( \rho_Q(\omega, k) \rho_{\bar{Q}}(E - \omega, k) [1 - f^Q(\omega) - f^{\bar{Q}}(E - \omega)] \right. \\ \left. + \rho_Q(\omega, k) \rho_Q(E + \omega, k) [f^Q(\omega, k) - f^Q(E + \omega, k)] \right) . \quad (5)$$

The first term characterizes the standard uncorrelated  $Q\bar{Q}$  propagation, while the second term (arising from negative-energy contributions) represents  $Q \rightarrow Q$  (or  $\bar{Q} \rightarrow \bar{Q}$ ) scattering which is nothing but the widely discussed zero-mode contribution to quarkonium correlators [13,14]. The scattering effect is encoded in the medium modifications of the single-quark spectral function, and thus intimately related to HQ transport. In the vector channel ( $\alpha=V$ ), the  $\mu\nu = 00$  component represents the density-density correlation ( $j_0$ : density) which in the static limit gives the HQ-number susceptibility,

$$\chi_c(T) = - \frac{\partial^2 \Omega}{\partial \mu_c^2} = \frac{\partial n_c}{\partial \mu_c} = \frac{1}{T} \int_0^\infty \frac{dE}{2\pi} \frac{2}{1 - \exp(-E/T)} \rho_V^{00}(E) , \quad (6)$$

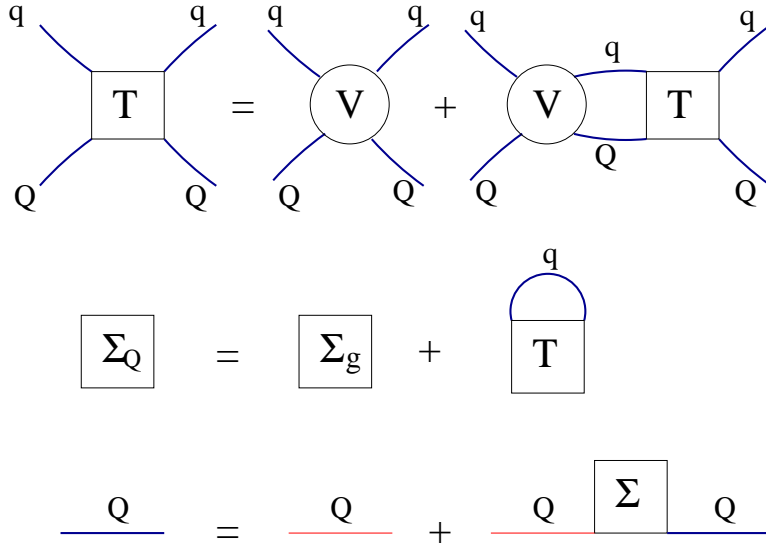


Fig. 2. Selfconsistent Brueckner problem for heavy quarks in the QGP: the heavy-light quark  $T$ -matrix (upper panel) figures into the calculation of the HQ selfenergy (middle panel) and propagator (lower panel), which in turn enters into the 2-particle propagator of the  $T$ matrix.

which is also governed by the zero mode.

The HQ spectral function is determined by the HQ selfenergy in the QGP,  $\Sigma_Q$ , as

$$\rho_Q(\omega, k) = \frac{-1}{\omega_Q(k)} \text{Im} \frac{1}{\omega - \omega_Q(k) - \Sigma_Q(\omega, k)} , \quad (7)$$

cf. the lower panel of Fig. 2. The selfenergy receives contributions from the interactions of the heavy quark with the heat-bath particles,  $\Sigma_Q \sim \int f^q T_{qQ}$ , but also from possible condensate remnants, especially gluon condensates (recall that the string tension,  $\sigma$ , seems to survive above  $T_c$ ), as illustrated in the middle panel of Fig. 2. Following the arguments given in the Introduction, the  $T$ -matrix approach may also apply to heavy-light interactions. In this case one can establish a selfconsistent Brueckner scheme in which quarkonium and open heavy-flavor interactions follow from the same potential (the construction of such a potential will be discussed below). Heavy-quark rescattering in the QGP is, of course, at the origin of its transport properties. The large HQ mass implies that momentum transfers are small compared to its thermal momenta,  $q \ll p_{\text{th}}$ . This leads to a Brownian motion picture with a Fokker-Planck equation for the time evolution of the HQ distribution function, schematically given by

$$\frac{\partial f}{\partial t} = \gamma \frac{\partial(pf)}{\partial p} + D \frac{\partial^2 f}{\partial p^2} , \quad \gamma p \sim \int f^q |T_{Qq}|^2 (1 - \cos \theta) . \quad (8)$$

The thermal relaxation rate,  $\gamma$ , is closely related to the scattering rate  $\Gamma_Q = -2 \text{Im} \Sigma_Q$ ; while the latter is computed with the forward scattering amplitude, the former includes a weight with the scattering angle,  $\theta$ , signifying the effect of isotropization.

Let us briefly discuss the construction of the interaction potential,  $\mathcal{V}$ , in Eq. (4). Originally it was hoped to extract it model-independently from IQCD measurements of the HQ free energy at finite  $T$  (right panel of Fig. 1), in analogy to the vacuum case (left

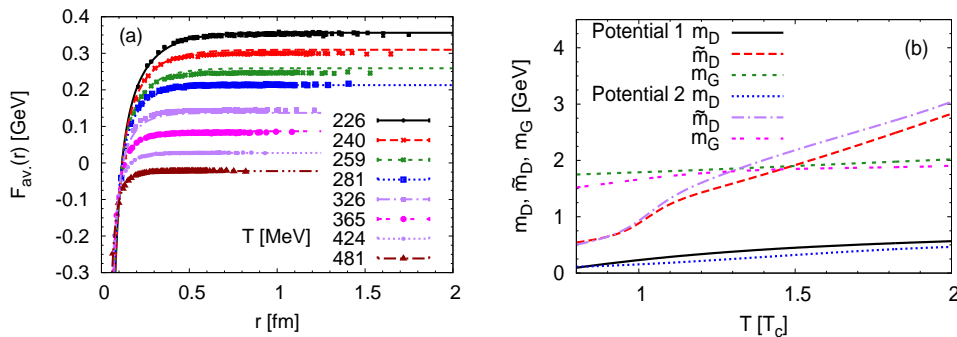


Fig. 3. Color-average  $Q\bar{Q}$  free energy at finite  $T$  (left panel) as computed in  $N_f = 2+1$  IQCD (symbols) and pertinent fits [11] using the “Coulomb+string” ansatz, Eq. (9). The  $T$ -dependence of the fit parameters is displayed in the right panel for 2 different IQCD inputs [16,17]. In both cases, the  $T$ -dependence of  $\alpha_s \simeq 0.28 - 0.32$  turns out to be weak. (Figures reproduced with permission from [11].)

panel of Fig. 1). However, at finite  $T$ , the entropy contribution in  $F = U - TS$  causes an ambiguity as to whether the free ( $F$ ) or internal energy ( $U$ ) should be used. This problem is related to the interplay of time scales for the HQ interaction and for the thermal relaxation of the medium, with  $U$  and  $F$  as limiting cases. On the other hand, we note that both  $F$  and  $U$  are computed from thermal expectation values, as differences between a system with and without an embedded  $Q\bar{Q}$  pair. A more rigorous approach should therefore start from (an ansatz for) a “bare” potential (figuring into the  $T$ -matrix equation) and then calculate the free (and internal) energies using suitable many-body techniques. The resulting “zero-point” functions ( $F$ ,  $U$ ) can then be compared to IQCD data and the input 4-point function (potential) tuned for optimal agreement. The thus obtained potential can be employed to calculate heavy-quark and -quarkonium properties in the QGP as described above.

The free and internal energies are believed to represent limiting cases bracketing the uncertainty in potential models. Instead of a functional parameterization of the lattice results a field-theoretic approach accounting for the two main components of the potential [15] has been proven very useful. With an ansatz for the effective Coulomb + confining propagators (including couplings),

$$D_{00}(k; T) = \frac{\alpha_s^2}{k^2 + m_D^2} + \frac{m_G^2}{(k^2 + \tilde{m}_D^2)^2}, \quad (9)$$

four parameters characterizing the respective interaction strength ( $\alpha_s$ ,  $m_G$ ) and in-medium screening ( $m_D$ ,  $\tilde{m}_D$ ) can be adjusted to reproduce the finite- $T$  color-average free energy from IQCD fairly well (see Fig. 3). To improve the applicability in the scattering regime a Breit correction as known from electrodynamics [18] has been introduced,  $V_{\text{Coul}} \rightarrow V_{\text{Coul}}(1 - \vec{v}_1 \cdot \vec{v}_2)$ , accounting for the magnetic current-current interaction. This modification renders the Coulomb potential “minimally” Poincaré invariant [19] and the high-energy limit of the  $T$ -matrix consistent with the tree-level perturbative QCD (pQCD) result [11]. Note that this extension only applies to a Lorentz-vector interaction (Coulomb term), not to the scalar confining term. It thus requires the explicit decomposition as given by the field-theoretic ansatz, Eq. (9). Further systematic improvements, e.g., scrutinizing the uncertainty of retardation effects, need yet to be performed. Com-

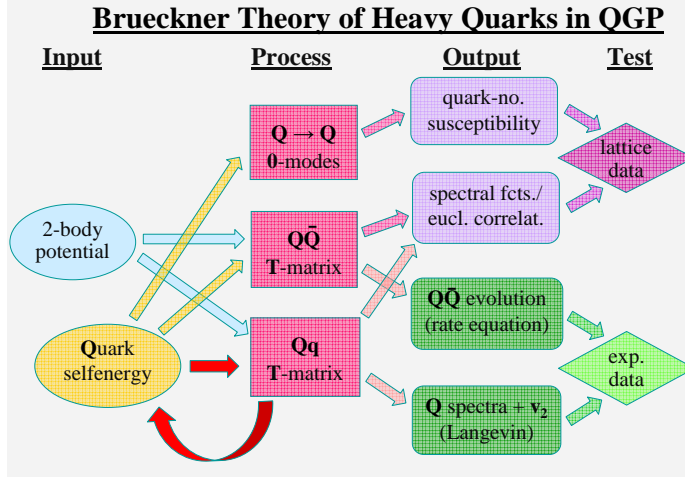


Fig. 4. Flow chart for a many-body approach to describe properties to heavy quarks and quarkonia in the QGP with applications to lQCD and heavy-ion data.

parisons to EFT approaches at finite  $T$  [20] could also prove useful, even though they are usually based on perturbative scale hierarchies which are problematic for the confining term. Interesting results are also emerging from lattice simulations of classical Yang-Mills theory [21], supporting the importance of nonperturbative effects.

### 3. Brueckner Theory of Heavy Flavor in QGP

In Fig. 4 we display a flow chart envisioning a possible implementation of Brueckner theory for heavy quarks in the QGP. Starting from an ansatz for the bare  $Q\bar{Q}$  potential (with suitable corrections and extensions to the heavy-light sector), two-body scattering amplitudes are readily calculated. From the heavy-light  $T$ -matrix one obtains a HQ selfenergy, which has to be iterated for selfconsistency for use in the final  $T$ -matrices. On the one hand, the latter are employed to compute spectral and correlation functions, susceptibilities and free/internal energies (not shown), all of which can be constrained by lattice “data” (and used to narrow down the input potential). On the other hand, one calculates HQ transport coefficients and quarkonium properties (masses, lifetimes, dissociation temperatures) which are readily implemented into phenomenological descriptions of URHICs (e.g., Langevin simulations or rate equations in a hydrodynamically evolving bulk medium) and checked against experiment [22–27].

As an example we show in Figs. 5 and 6 results from a recent selfconsistent Brueckner calculation including off-shell width effects in the HQ propagators [12]. When using the lQCD internal energy as input potential, one finds HQ widths of considerable magnitude, reaching up to  $\Gamma_Q \simeq 0.1\text{--}0.2\text{ GeV}$  for on-shell charm quarks. When implemented into the charmonium  $T$ -matrix, the ground-state ( $\eta_c, J/\psi$ ) melting temperature (estimated from the disappearance of the bound-state peak) is found to be around  $1.5 T_c$ , significantly smaller than in calculations neglecting width effects ( $\sim 2 T_c$ ). The resulting euclidean correlators, including zero modes according to Eq. (5), show fair agreement with lQCD

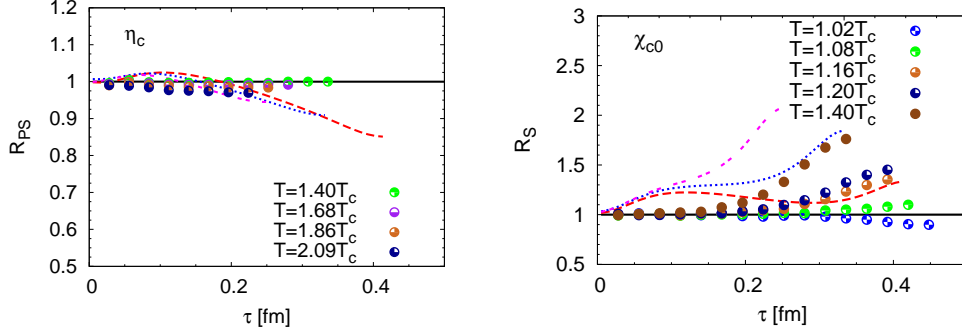


Fig. 5. Euclidean charmonium correlators ( $G_\alpha$ ), normalized to the ones with vacuum spectral function but with finite- $T$  kernel,  $R_\alpha(\tau) \equiv G_\alpha(\tau)/G_\alpha^{\text{vac}*}(\tau)$ . The  $T$ -matrix results at  $T=1.2, 1.5$  and  $2T_c$  (dashed, dotted and double-dashed curves) [12] are compared to 2-flavor IQCD computations [28] in the pseudoscalar ( $\eta_c$ ) channel (left; no zero-mode) and scalar ( $\chi_{c0}$ ) channel (right; including zero modes).

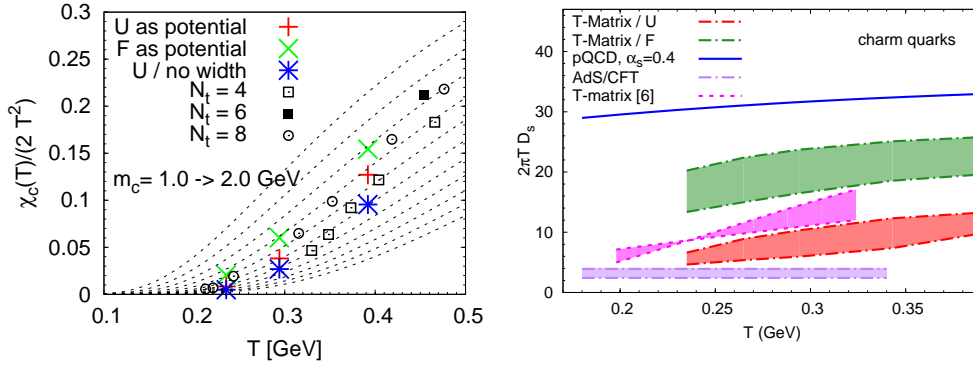


Fig. 6. Left: charm-quark susceptibility (normalized to twice the free massless limit) from selfconsistent Brueckner calculations with  $U$  or  $F$  potentials (colored symbols), IQCD (squares, circles) [29] and non-interacting  $c$ -quarks with masses  $m_c=1\text{--}2$  GeV in steps of  $0.1$  GeV (dashed lines, top down). Right: spatial diffusion coefficient for  $c$  quarks from the  $T$ -matrix with  $U$  (pink [22] and red bands [11]) and  $F$  potentials (green band) [11], LO pQCD (solid line) and AdS/CFT matched to QCD [30] (lower band).

data (see Fig. 5), even though quantitative improvements are certainly warranted. Still within the same framework, the HQ susceptibility, Eq. (6), has been computed and compared to IQCD data (left panel of Fig. 6). For this quantity the width effects lead to an appreciable increase over the zero-width limit, providing better overlap with IQCD data. The results of a calculation with the free energy as potential generate a larger  $\chi_c$ , since for  $F_{Q\bar{Q}}$  the in-medium HQ mass correction,  $\Delta m_Q = F_{Q\bar{Q}}(r \rightarrow \infty)$ , is about  $0.3$  GeV smaller than for  $U_{Q\bar{Q}}$ . Finally, the resulting spatial HQ diffusion coefficients, computed from the selfconsistent heavy-light  $T$ -matrix within a Fokker-Planck equation (8) with  $D_s = T/(m_Q\gamma)$ , are displayed in Fig. 6. When using the  $U$ -potential,  $D_s$  turns out to be a factor of 3-5 smaller (indicating stronger coupling) compared to pQCD. Toward  $T_c$ , the values are not very far from the strong-coupling limit represented by AdS/CFT (close to  $T_c$  the  $T$ -matrix is not yet reliable, e.g., due to the lack of coupled channels such as  $D\bar{D}$ ). With  $F$  as potential  $D_s$  is roughly in between the  $U$ -scenario and pQCD.

## 4. Conclusions

We have argued that nonperturbative elastic interactions are key to understanding low-momentum interactions of heavy quarks in the QGP. A potential-based  $T$ -matrix approach is, in principle, capable of connecting heavy quarkonium and heavy-flavor transport physics. This opens a rich arsenal of constraints from thermal lattice QCD on quantities which directly relate to phenomenological applications in URHICs. Many open questions remain, e.g., a proper potential definition or the role of correlations near  $T_c$  and nonperturbative  $Q$ -gluon interactions. Systematically addressing these issues will be essential for a full exploitation of upcoming high-precision heavy-flavor measurements at RHIC, LHC and FAIR.

**Acknowledgment** I thank the organizers of ICPAQGP10 for a very stimulating meeting. I am indebted to my collaborators on the presented topics, D. Cabrera, V. Greco, H. van Hees, F. Riek and X. Zhao. This work has been supported by the U.S. National Science Foundation under grant no. PHY-0969394 and by the A.v. Humboldt Foundation (Germany).

## References

- [1] F. Karsch, E. Laermann and A. Peikert, Nucl. Phys. **B605** (2001) 579.
- [2] O. Kaczmarek and F. Zantow, Phys. Rev. D **71** (2005) 114510.
- [3] R. Rapp, D. Blaschke and P. Crochet, Prog. Part. Nucl. Phys. **65**, 209 (2010).
- [4] P. Braun-Munzinger and J. Stachel, LANL eprint arXiv:0901.2500 [nucl-th].
- [5] L. Kluberg and H. Satz, LANL eprint arXiv:0901.4014 [hep-ph].
- [6] R. Rapp and H. van Hees, LANL eprint arXiv:0903.1096 [hep-ph].
- [7] R. Redmer, Phys. Rep. **282** (1997) 35.
- [8] A. Mocsy and P. Petreczky, PoS **LAT2007** (2007) 216.
- [9] M. Mannarelli and R. Rapp, Phys. Rev. C **72** (2005) 064905.
- [10] D. Cabrera and R. Rapp, Phys. Rev. D **76** (2007) 114506.
- [11] F. Riek and R. Rapp, Phys. Rev. C **82** (2010) 035201.
- [12] F. Riek and R. Rapp, LANL eprint arXiv:1012.0019 [nucl-th].
- [13] G. Aarts and J.M. Martinez Resco, Nucl. Phys. **B726** (2005) 93.
- [14] T. Umeda, Phys. Rev. D **75** (2007) 094502.
- [15] E. Megias, E. Ruiz Arriola and L.L. Salcedo, JHEP **01** (2006) 073; Phys. Rev. D **75** (2007) 105019.
- [16] O. Kaczmarek, PoS **CPOD07** (2007) 043; and priv. comm.
- [17] P. Petreczky and K. Petrov, Phys. Rev. D **70** (2004) 054503; P. Petreczky, priv. comm.
- [18] G.E. Brown, Philos. Mag. **43** (1952) 467.
- [19] N. Brambilla, D. Gromes and A. Vairo, Phys. Lett. **B576** (2003) 314.
- [20] N. Brambilla, J. Ghiglieri, A. Vairo and P. Petreczky, Phys. Rev. D **78** (2008) 014017.
- [21] M. Laine, G.D. Moore, O. Philipsen and M. Tassler, JHEP **0905** (2009) 014.
- [22] H. van Hees, M. Mannarelli, V. Greco and R. Rapp, Phys. Rev. Lett. **100** (2008) 192301.
- [23] P.B. Gossiaux and J. Aichelin, Phys. Rev. C **78** (2008) 014904.
- [24] W.M. Alberico, A. Beraudo, A. De Pace *et al.*, LANL eprint arXiv:1011.0400 [hep-ph].
- [25] S.K. Das and J.-e. Alam, these proceedings, LANL eprint arXiv:1101.3385 [nucl-th].
- [26] X. Zhao and R. Rapp, Phys. Rev. C **82** (2010) 064905.
- [27] Y. Liu, B. Chen, N. Xu and P. Zhuang, LANL eprint arXiv:1009.2585 [nucl-th].
- [28] G. Aarts, C. Allton, M.B. Oktay, M. Peardon and J.I. Skullerud, Phys. Rev. D **76** (2007) 094513.
- [29] P. Petreczky, P. Hegde and A. Velytsky [RBC-Bielefeld Collaboration], PoS **LAT2009** (2009) 159.
- [30] S.S. Gubser, Phys. Rev. D **76** (2007) 126003.